Section 1
PROGRESS IN LASER FUSION

1.A The Effect of Photoelectric Fluorescence on the Formation of X-Ray Absorption Lines in Laser-Plasma Experiments

In laser-plasma experiments, conditions in an embedded layer in a target shell can be inferred from the spectral attenuation of x-ray continuum radiation by the layer.[1] In such experiments, absorption lines are formed by 1s–2p absorption transitions in helium-like through fluorine-like species of certain ions in the layer to be diagnosed. The areal density of each species can be inferred from the attenuation in the spectrum within its respective band, provided the average 1s–2p absorption cross sections for each species are known and provided competing line-forming mechanisms are taken into account. In photoelectric fluorescence, which is one such potentially important competing mechanism, the formation of a 1s vacancy by photoionization is followed by 2p–1s spontaneous emission within the same spectral range as the 1s–2p absorption band of the same ion. The importance of photoelectric fluorescence depends on the supply of ionizing photons, which is sensitive to the design of the experiment. This process should be considered when analyzing experiments where the continuum is hardened by high core temperatures, by opacity effects, or by core components that radiate efficiently at ionizing energies.

Introduction

In absorption spectroscopy, absorption features impressed on the spectrum of a continuum background source are interpreted in terms of conditions in an absorbing foreground medium. If the opacity per ion caused by a particular transition beginning from some initial state is known, then

the areal density (i.e., the path integral of the density along the path of the continuum propagation) of ions in that state within the absorbing medium can be inferred from the attenuation of the background continuum caused by that transition.[2,3] If the relative abundance of ion species can be determined in this way, then temperature in the absorbing medium can also be inferred from the observed state of ionization, which can be modeled in terms of temperature and density.[3]

In x-ray spectra from inertial confinement fusion experiments and other laser-plasma experiments, the absorption features of interest are typically arrays of 1s–2p lines from the ground configuration and from certain low-lying excited configurations of L-shell ion species, fluorine-like through helium-like. The arrays from each species form a distinct band of absorption where the individual lines are usually not resolved. We consider here the contribution of photoelectric fluorescence to reducing the net attenuation of the continuum within each of these 1s–2p absorption bands.

Photoelectric fluorescence is the 2p–1s emission that follows the formation of a 1s vacancy by photoionization. These emission transitions are inverses of the transitions that form the absorption arrays, so fluorescence reduces the apparent line absorption. This emission is equivalent to the "K-alpha" emission lines caused by K-shell ionization as a result of the impact of suprathermal electrons[4] or photons[5] formed in the plasma corona of a target as it is illuminated by high-intensity infrared laser light.

The importance of photoelectric fluorescence will be estimated and expressed in terms of atomic parameters and local plasma conditions within a volume element by comparing local absorption and emission rates, rather than in the context of specific ions in a specific experimental geometry. In this way, the ranges of conditions and atomic parameters where photoelectric fluorescence has potential importance can be more easily recognized. Approximate formulae for atomic rates with explicit parameter dependences are used. The results show that typical continua from the cores of imploded targets can produce enough emission by photoelectric fluorescence to compete with absorption by photoexcitation and that quantitative interpretation of absorption spectra must take this effect into account.

In laser-driven, direct-drive inertial confinement experiments,[6] compression at the center of the target creates conditions of high density and temperature that produce a burst of continuum radiation near the time of peak compression. This radiation passes through the imploded shell of the target on its way to the spectrograph. This shell remnant usually remains within the range of temperatures where light elements in the neighborhood of chlorine (e.g., silicon through calcium) would be ionized to fluorine-like through helium-like states.[3] This temperature is typically of the order of a few hundred electron volts, which is much cooler than the temperatures in the coronal region and in the compressed core. Since these ions have partially vacant L shells, absorption lines can be imprinted on the passing background continuum by inner-shell absorption transitions of the kind 1s–2p. These

absorbing elements either occur naturally in the shell material itself, e.g., silicon in glass,[2] or they can be introduced as additives or deposited as a thin concentric layer inside the shell.[3]

Emission and Absorption

The probability that spontaneous emission will occur in an ion following the removal of a 1s electron is called the K-shell fluorescence efficiency ω_K.[7] In an isolated ion, Auger autoionization[8] is the other possible outcome, and ω_K is the branching ratio between Auger autoionization and spontaneous emission

$$\omega_K = \frac{A_{21}}{A_{21} + A_{\text{auto}}}, \tag{1}$$

where A_{21} and A_{auto} are the spontaneous emission and Auger autoionization rates, respectively.

The fraction of 1s vacancies formed by photoionization that lead to line emission is small, since $\omega_K << 1$ for low-Z species.[9] However, the supply of ionizing photons can be large enough, compared to the number of excitation photons within the 1s–2p absorption band, to yield a significant competing emission. The K-shell fluorescence efficiency also gives the probability of re-emission when a 1s vacancy is created by photoexcitation in the formation of absorption lines. This re-emission decreases the depth of the absorption lines, but the fraction of excitations that end in re-emission is generally neglected, again, since $\omega_K << 1$. Photoexcitation of higher transitions, such as 1s–3p, creates 1s vacancies that also decay, in part, via the 2p–1s radiative transitions, but this is a smaller effect and will be ignored here.

The fluorescence efficiencies generally quoted are values appropriate for isolated atoms or ions. In plasmas, electron collisional transitions from one autoionizing state to another can affect the fluorescence efficiency.[10] At higher densities ($n_e \sim 10^{24}$; see the following), the 1s vacancy can also be filled by radiative or collisional recombination or by collisional de-excitation,[11] and as these rates become comparable with spontaneous emission, fluorescence is quenched.

Rates and Approximations

The screened hydrogenic approximation is applicable to highly ionized species since spectator electrons have a smaller effect on electron orbits than the central nuclear charge, particularly for K-shell orbits that are largely internal to the spectator electrons and are thus least affected by them. This approximation is adequate for calculating a correction factor for the absorption. The explicit dependence of screened-hydrogenic rate expressions on atomic parameters is useful in expressing the importance of photoelectric fluorescence over a broad range of atomic parameters and local conditions.

Photoexcitation

The absorption cross section of a given transition i can be written in the form $\sigma_i \phi_i(\nu)$, where $\phi_i(\nu)$ is the line profile, normalized to unity with respect to integration over frequency ν, and where σ_i is the frequency-integrated cross section of the transition. The attenuated intensity $I(\nu)$ remaining after the incident background continuum intensity I_0 passes through a homogeneous layer of thickness Δr of material with a number density N_I of the absorbing species is

$$\ln\left[\frac{I_0}{I(\nu)}\right] = N_I \Delta r \, \sigma_i \phi_i(\nu) \ , \tag{2}$$

where

$$\sigma_i = \frac{\pi e^2}{m_e c} f \tag{3}$$

and f is the absorption oscillator strength of the transition.

In the simplest interpretation of this attenuation, neglecting instrumental broadening, foreground emission, etc., the areal density of the absorbing species $N_I \Delta r$ can be obtained from the integrated attenuation and from the integrated cross section σ_i, using

$$\int \ln\left[\frac{I_0}{I(\nu)}\right] d\nu = N_I \Delta r \sigma_i \ . \tag{4}$$

Note that this expression is independent of the line profile, which need not be considered further in this interpretation.[3]

The average absorption cross section for each species is obtained by averaging the cross sections of all 1s–2p transitions from all possible initial configurations, weighted according to the statistical weights of the initial states. The relevant species are helium-like through fluorine-like, and up to three initial configurations are possible, (1) $1s^2 2s^2 2p^n$ (ground), (2) $1s^2 2s 2p^{n+1}$ (singly excited), and (3) $1s^2 2p^{n+2}$ (doubly excited), subject to the restriction that there be no more than six 2p electrons in the final state. The average photoexcitation cross sections for each configuration used here are screened hydrogenic results scaled from the helium-like cross section σ_{He}, according to

$$\sigma_i = \sigma_{He}\left(1 - P_{2p}/6\right), \tag{5}$$

where P_{2p} is the occupation number of the 2p subshell. Even though the spectator charge in these ions varies from one to eight electrons (nearly half

the nuclear charge, in the case of argon), this approximation works very well, particularly for the relative absorption strengths of the configurations of a given species.[12]

The unresolved 1s–2p transition arrays from each contributing configuration coincide closely, so it suffices to treat them as a single feature with an effective absorption strength obtained by averaging over the three possible initial configurations. At typical shell temperatures, the low-lying $1s^2(2s+2p)^n$ configurations are linked by 2s–2p transitions that are readily excited by electron collisions. We assume, then, that these configurations are populated according to their statistical weights. At temperatures where these species will have non-negligible populations, this is a good approximation to the more correct weighting using the temperature-dependent Boltzmann ratio.[12,13]

The vacancy fractions and statistical weights for the L-shell configurations needed to evaluate Eq. (4) and to perform the appropriate configuration averaging are given in Table 46.I.

Photoionization

The photoionization rate is calculated in the screened hydrogenic approximation[14] assuming the Kramers cross section[15] per electron in principal level n

$$\sigma_{n,z}(\nu) = \frac{64\pi^4 e^{10} m_e z^4}{3\sqrt{3} h^6 c \nu^3 n^5} g_{PI}(z,n,\nu) , \tag{6}$$

with the Gaunt factor of Menzel and Pekeris[15]

$$g_{PI}(z,n,\nu) = 1 - 0.1728 \left(\frac{h\nu}{I_H z^2}\right)^{1/2} \left[\frac{2}{n^2}\left(\frac{I_H z^2}{h\nu}\right) - 1\right], \tag{7}$$

where I_H is the ground-state ionization energy of hydrogen, I_H = 13.6 eV.

Fluorescence Efficiency

Fluorescence efficiency for K-alpha emission from neutral atoms is well documented, theoretically and experimentally, but relatively little can be found on ionized atoms. We can infer fluorescence efficiencies for ions from the neutral values by the model of McGuire,[17] which compares well with Bhalla and Tunnell[18] for lithium-like argon and with McGuire for the L-shell ions of aluminum. In this model, the radiative decay probability of an ion with a K-shell vacancy $A_r P_{2p}$ is written to scale with P_{2p}, the number of 2p electrons, and the Auger ionization probability $A_a P_{2p}(P_{2p}-1)$ is written to scale with the number of pairs of 2p electrons. The latter product reflects the joint probability of one 2p electron decaying and transfering its energy to another 2p electron. The fluorescence efficiency, in terms of these rates, is

$$\omega_K = \frac{A_r P_{2p}}{A_r P_{2p} + A_a P_{2p}\left(P_{2p} - 1\right)} , \tag{8}$$

which is appropriate for isolated ions.

High-Density Effects on Fluorescence Efficiency

Fluorescence efficiency is usually derived for the case of an isolated ion, but local density of electrons can introduce additional processes that alter or quench it. It has been shown, for example, that electron collisions can rearrange the L-shell configuration of an ion quickly enough after the formation of a K-shell vacancy to affect the branching between autoionization and spontaneous emission.[10] Estimates of other corrections to the fluorescence efficiency of an isolated ion, given by Eq. (1), can be obtained by using the following approximate expressions for the processes of interest.

The rate of spontaneous emission from the $n = 2$ shell to the $n = 1$ shell is given by

$$A_{21} = 4.34 \times 10^7 \left(\sec^{-1}\right) f_{21} \left(\frac{\Delta E}{\mathrm{eV}}\right)^2 , \tag{9}$$

where ΔE is the transition energy, $f_{21} = 0.05125 \times P_2$ is the oscillator strength (based on the scaled hydrogenic result),[19] and P_2 is the number of L-shell electrons.

For collisional de-excitation[20]

$$C_{21} = 4.50 \times 10^{-6} \left(\sec^{-1}\right) \frac{n_e f_{21}}{\left(\frac{\Delta E}{\mathrm{eV}}\right)\left(\frac{T}{\mathrm{eV}}\right)^{1/2}} . \tag{10}$$

The rate coefficient α_3 for collisional 3-body recombination to level n of the species of charge Z to form the species of charge $Z-1$ is obtained from the detailed balance relationship

$$\alpha_3 = \frac{g_{Z-1}}{g_Z} \frac{n_e}{2} \left(\frac{h^2}{2\pi m_e kT}\right)^{3/2} e^{\chi_n / kT} S_n , \tag{11a}$$

where g_Z and g_{Z-1} are the respective statistical weights of the relevant species, and from S_n, the rate coefficient of collisional ionization from level n[21]

$$S_n = 3.0 \times 10^{-6} \left(\sec^{-1}\right) \frac{\left(\frac{n_e}{\mathrm{cm}^{-3}}\right) P_n Ei\left(\frac{\chi_n}{T}\right)}{\left(\frac{T}{\mathrm{eV}}\right)^{3/2} \left(\frac{\chi_n}{T}\right)} . \tag{11b}$$

The exponential integral $Ei(x)$ is given by the rational approximation

$$e^x Ei(x) \cong \frac{1.25}{1.00+1.25x} . \tag{11c}$$

The rate coefficient of K-shell radiative recombination is given by[22]

$$\alpha_r = 5.20\times10^{-14}\left(\sec^{-1}\right)\left(\frac{n_e}{\mathrm{cm}^{-3}}\right)Z\left(1-\frac{P_{1s}}{2}\right)\left(\frac{\chi}{T}\right)^{3/2} e^{\chi/T} Ei\left(\frac{\chi}{T}\right) . \tag{12}$$

The rate coefficients in Eqs. (9)–(12) are written with the electron density n_e in electrons per cubic centimeter, and with the ionization energies χ, the excitation energy ΔE, and the electron temperature T all in electron volts. With these expressions, a corrected fluorescence efficiency can be written that includes the effects of radiative and collisional recombination and collisional de-excitation,

$$\omega_K^* = \frac{\omega_K}{1+(C_{21}+\alpha_3+\alpha_r)(\omega_K/A_{21})} , \tag{13}$$

where

$$\frac{\omega_K C_{21}}{A_{21}} = 9.60\times10^{-2}\frac{\left(\frac{\omega_K}{0.25}\right)\left(\frac{n_e}{10^{24}\,\mathrm{cm}^{-3}}\right)}{\left(\frac{h\nu_0}{3\ \mathrm{keV}}\right)^3\left(\frac{T}{100\ \mathrm{eV}}\right)^{1/2}} , \tag{14}$$

$$\frac{\omega_K \alpha_3}{A_{21}} = 3.88\times10^{-3}\frac{\left(\frac{\omega_K}{0.25}\right)\left(\frac{n_e}{10^{24}\,\mathrm{cm}^{-3}}\right)^2}{\left(\frac{h\nu_0}{3\ \mathrm{keV}}\right)^4\left(\frac{T}{100\ \mathrm{eV}}\right)P_2} , \tag{15}$$

and

$$\frac{\omega_K \alpha_r}{A_{21}} = 0.0344\frac{\left(\frac{\omega_K}{0.25}\right)\left(\frac{n_e}{10^{24}\,\mathrm{cm}^{-3}}\right)\left(\frac{Z}{16}\right)}{\left(\frac{h\nu_0}{3\ \mathrm{keV}}\right)^{3/2}\left(\frac{T}{100\ \mathrm{eV}}\right)^{1/2}P_2} \tag{16}$$

These correction terms are expressed in terms of scaling parameters normalized to values appropriate for argon at a nominal temperature of 200 eV and a nominal electron density of $10^{24}\,\mathrm{cm}^{-3}$. Under these conditions, the correction to the fluorescence efficiency is small. Should the shell reach significantly higher densities, fluorescence could actually be quenched, thus greatly simplifying the task of including it in a model of the absorption signal. These preliminary results show that careful modeling of all the processes that contribute to the fluorescence efficiency can be important to the modeling of the 1s–2p absorption signal.

Table 46.I: Average parameters for the configurations of chlorine ions.

Configuration	Weighted Oscillator Strength (gf)	Statistical Weight	2p Vacancy	Species Average 2p Vacancy	Average gf Per Unit Vacancy
Helium-like					
$1s^2$	0.882	1	6	6.00	0.822
Lithium-like					
$1s^22s$	1.559	2	6	5.25	0.788
$1s^22p$	3.864	6	5		
Beryllium-like					
$1s^22s^2$	0.745	1	6	4.50	0.780
$1s^22s2p$	7.594	12	5		
$1s^22p^2$	7.484	15	4		
Boron-like					
$1s^22s^22p$	3.657	6	5	3.75	0.770
$1s^22s2p^2$	14.705	30	4		
$1s^22p^3$	7.262	20	3		
Carbon-like					
$1s^22s^22p^2$	7.09	15	4	3.00	0.759
$1s^22s2p^3$	14.230	40	3		
$1s^22p^4$	3.500	15	2		
Nitrogen-like					
$1s^22s^22p^3$	6.867	20	3	2.25	0.747
$1s^22s2p^4$	6.867	30	2		
$1s^22p^5$	0.676	6	1		
Oxygen-like					
$1s^22s^22p^4$	3.288	15	2	1.50	0.723
$1s^22s2p^5$	1.317	12	1		
$1s^22p^6$	0.0	1	0		
Fluorine-like					
$1s^22s^22p^5$	0.635	6	1	0.75	0.707
$1s^22s2p^6$	0.0	2	0		

TC2968

Results and Discussions

The effect of interest is the filling of absorption lines by fluorescence emission. A measure of the importance of the photoelectric fluorescence effect, relative to photoexcitation, can be expressed in terms of the local rates of emission and absorption, which are functions of local plasma conditions. One such measure is the number of fluorescent photons emitted for each photon absorbed and destroyed within the 1s–2p transition band of a given ion species

$$\left(\frac{\text{fluorescence}}{\text{absorption}}\right) = \frac{\omega_K N_{Z-1} \int_{\chi_0/h}^{\infty} \frac{I(\nu)}{h\nu} \sigma_{K,Z-1}(\nu) d\nu}{(1-\omega_K) N_Z \frac{I(\nu_0)}{h\nu_0} \sigma_{i,z}} \quad . \tag{17}$$

The K-shell photoionization rate is determined by the cross section $\sigma_{K,Z-1}$ for the removal of a K-shell electron from the species of charge $Z-1$ due to photons above the ionization energy χ_{Z-1}. The form of the local radiation continuum $I(\nu)$ and the relative populations of ions of the absorbing species N_Z and ions of the photoionization parent species N_{Z-1} must be specified. The species of charge $Z-1$ is photoionized into excited states of the absorbing species of charge Z that subsequently radiate into the absorption band, in direct competition with the formation of the absorption line. The $(1-\omega_K)$ factor multiplying the photoexcitation rate in the denominator represents a correction for re-emission.

The continuum is characterized by a temperature T and by an index q that spans spectra from a free-free continuum ($q = 0$) to the high-energy Wien limit of a blackbody ($q = 3$)

$$I(\nu) \sim \nu^q e^{-\tau_0 (\nu_0/\nu)^3} e^{-h\nu/kT} \quad . \tag{18}$$

An attenuation factor is included that represents the modification of the continuum due to a bound-free absorbing layer. The optical depth of this absorber is τ_0 at line center and extrapolates to lower opacity at higher energies where photoionization takes place, thus hardening the continuum and enhancing fluorescence relative to photoexcitation.

In Fig. 46.1, the ratio $F(T, q, \tau_0)$ of the number of photoelectric fluorescence photons emitted to the number of photoexcitation photons absorbed within the total 1s–2p transition signal of the boron-like species of argon is plotted as a function of the continuum temperature for various continua, assuming equal numbers of boron-like and carbon-like ions. The fluorescence filling ratio scales to other ions as

$$\left(\frac{\text{fluorescence}}{\text{absorption}}\right) \cong F(T,q,\tau_0) \frac{N_{Z-1}}{N_Z} \frac{\left(\frac{\omega_k}{0.25}\right)}{\left(\frac{1-\omega_k}{0.75}\right)\left(\frac{1-P_{2p}/6}{0.5}\right)} \quad . \tag{19}$$

The nominal $\omega_K = 0.25$ value for boron-like argon is estimated based on the value $\omega_K = 0.127$ for neutral argon[23] and the scaling suggested by Eq. (8). The set of solid curves is obtained from exponential continua typical of optically thin emission $q = 0$, and the dashed curves represent the high-energy Wien limit of the blackbody spectrum $q = 3$. Each curve within each set has been calculated for various values of the preabsorber optical depth ($\tau_0 = 0, 1, 2,$ and 3) at the line center. Absorbing layers of any optical depth can be considered, but beyond some point, the attenuation will make the absorption signal too small to be useful.

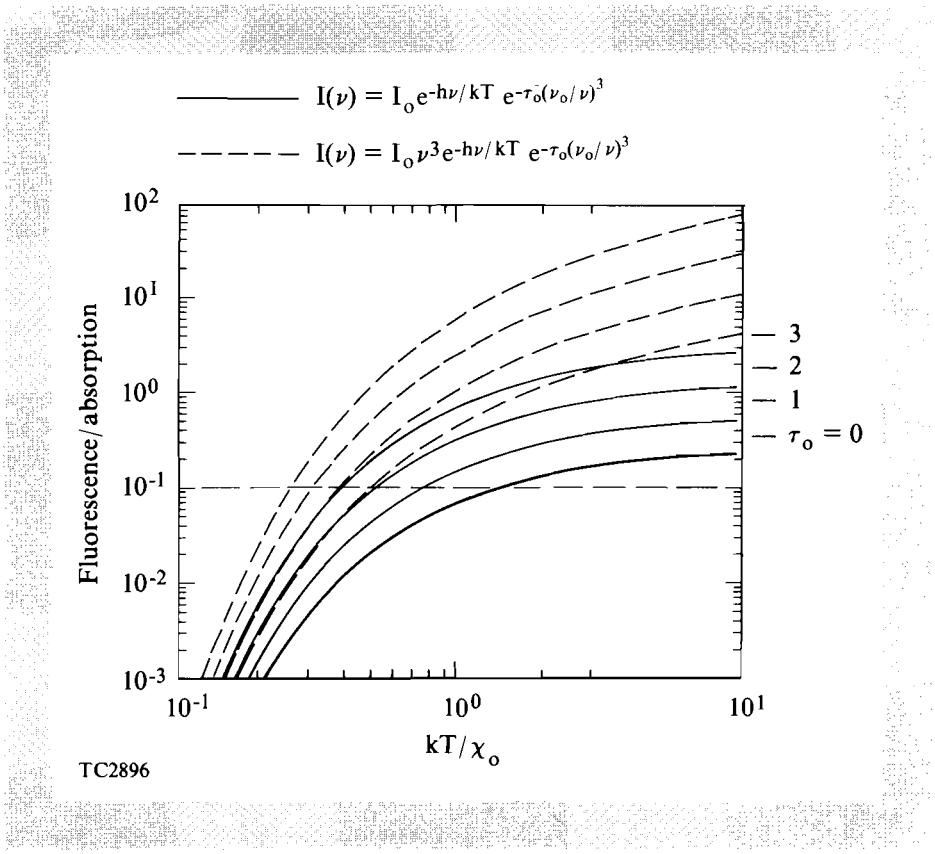

Fig. 46.1
The ratio of the number of photoelectric fluorescence photons emitted to the number of photoexcitation photons absorbed within the total 1s–2p transition band of the boron-like species of argon is plotted as a function of the continuum temperature for various continuum spectra. It is assumed that equal numbers of boron-like and carbon-like ions are present. The set of solid curves is obtained from exponential continua typical of optically thin emission, and the set of dashed curves represents the high-energy Wien limit of the blackbody spectrum. Each curve within the two sets has been calculated assuming that the continuum is filtered by a bound-free or free-free absorbing of optical depth τ_0 (0, 1, 2, and 3) at the line center. The marks by the right-hand axis give the high-temperature limit of the optically thin results.

Figure 46.1 shows that fluorescence can have an effect of 10% or more on the net absorption signal over a broad range of parameters, so it should be included in calculations involving absorption-line formation. It is also seen that fluorescent emission can fill the absorption lines only for continuum temperatures much higher than the ionization energy and/or for strong continuum hardening by an absorber. Hardening will be especially prominent for highly compressed targets having a high-Z absorbing layer, where the opacity is higher. Opacity will also be higher in lower-Z materials, such as carbon, if the absorbing layer is cool enough for bound-free-absorbing species to be abundant.

A special case arises when a high-Z fill gas, such as argon, is compressed with a radial temperature gradient. The central core can give rise to a strong continuum that produces absorption lines in the cooler, peripheral layer of the fill gas. The jump in the emission spectrum above the K-edge of, say, the helium-like ions will be efficient in producing photoionization in the peripheral layer. However, the absorption lines are located below the K-edge, where the continuum intensity is lower, which results in enhanced photoionization, relative to photoexcitation, as compared with the case of a smoother continuum spectrum.

Caution should be exercised in applying these results in the following instances: (a) The observation of K-alpha lines in emission need not be

interpreted as evidence of overwhelming fluorescence. This is because the continuum emitted by the outer, laser-heated target layer (especially if it is a high-Z layer) can excite K-alpha lines while propagating inwards. This could result in observable K-alpha emission lines without contributing to observable absorption lines. Figure 46.1 shows that local fluorescence-absorption ratios near and above unity are unlikely. For thin ($q = 0$) continua, this requires high temperatures ($kT > \chi_0$) and enough opacity hardening to obscure the signal substantially ($\tau_0 > 3$). (b) The comparison of local emission and absorption rates as an indication of the relative importance of fluorescence and absorption, i.e., the ratio given by Eq. (17), applies only to a representative sample of all the radiation escaping the plasma and may not conform to the measurements when, for example, the recorded spectrum is spatially resolved, especially if the continuum is emitted by a small, compressed core. The emission along the line of sight that traverses the center of the target under-represents the fluorescence. On the other hand, a line of sight that does not traverse the center may partly miss the absorption lines, but not the fluorescence emission. (c) The previously calculated ratio of fluorescence and absorption is valid when the absorption is weak enough not to reach saturation (i.e., depletion of the incident continuum photons). Since photoexcitation is a resonance effect, it will reach saturation before photoionization does. However, by the time saturation is reached, the absorption lines start to lose their diagnostic value and can at best be used to obtain a lower bound on the shell $\rho\Delta r$.

In deriving Eq. (17), it is assumed that the fluorescence spectrum is determined by the population distribution of L-shell ion species, the rate at which K-shell ionization and excitation produces K-shell vacancies in these ions, and the rate at which these vacancies decay. This requires the assumption that the K-shell fluorescence processes occur rapidly, before the ionization state of the newly formed [1s] ions, those with K-shell vacancies (e.g., $1s2s^n2p^m$), can redistribute. Such changes would alter the fluorescence spectrum. The distribution of L-shell configurations of the [1s] ions will evolve at a rate corresponding to the net difference in L-shell ionization and recombination rates. This net rate is proportional to the degree to which the [1s] ions are out of ionization equilibrium and is likely to be much less than the individual rates. In particular, the initial distribution of [1s] ions formed by ionization will be close to equilibrium because the parent $1s^2$ ions (e.g., $1s^22s^n2p^m$) would most likely be close to equilibrium and because the K-shell ionization rates change relatively little from species to species. The distribution of [1s] species formed by photoexcitation, on the other hand, could be skewed because the relevant cross sections are proportional to the L-shell vacancy fractions of the parent ions. What is likely to cause the distribution of [1s] species to relax before fluorescence could occur is, for example, L-shell radiative recombination, which determines the plasma ionization state over a wide range of conditions. At the same time, however, K-shell radiative recombination would quench the fluorescence at a comparable rate. A preliminary assessment, then, is that the fluorescence spectrum should not be altered by L-shell effects, except under circumstances that would quench the fluorescence altogether.

Conclusions and Summary

It is difficult to accurately predict the importance of an effect such as photoelectric fluorescence in a given experiment without full simulations. Nevertheless, the parameter dependences and scaling behaviors revealed in the simple calculation in this article should serve as a useful guide to anyone asking whether or not this effect is relevant to a particular experiment or simulation.

Even though other effects, such as inhomogeneities in temperature and density and the nonuniform sampling of the shell by a compact continuum source, can introduce comparable uncertainties and ambiguities into estimates of areal densities, the effect of the photoelectric fluorescence is systematic and should not be neglected.

ACKNOWLEDGMENT

This work was supported by the U.S. Department of Energy Division of Inertial Fusion under agreement No. DE-FC03-85DP40200 and by the Laser Fusion Feasibility Project at the Laboratory for Laser Energetics, which has the following sponsors: Empire State Electric Energy Research Corporation, New York State Energy Research and Development Authority, Ontario Hydro, and the University of Rochester.

REFERENCES

1. B. Yaakobi, R. L. McCrory, S. Skupsky, J. A. Delettrez, P. Bourke, H. Deckman, C. F. Hooper, and J. M. Soures, *Opt. Commun.* **34**, 213 (1980).
2. *Ibid.*; A. Hauer, in *Spectral Line Shapes,* edited by B. Wende (W. de Gruyter & Co., Berlin, 1981); D. K. Bradley, J. D. Hares, and J. D. Kilkenny, Rutherford-Appleton Laboratory, Annual Report No. RL-83-043, 1983, p. 5.4.
3. A. Hauer, R. D. Cowan, B. Yaakobi, O. Barnouin, and R. Epstein, *Phys. Rev. A* **34**, 411 (1986).
4. B. Yaakobi, I. Pelah, and J. Hoose, *Phys. Rev. Lett.* **37**, 836 (1976).
5. J. D. Hares, J. D. Kilkenny, M. H. Key, and J. G. Lunney, *Phys. Rev. Lett.* **42**, 1216 (1979); A. Hauer, W. Priedhorsky, and D. van Hulsteyn, *Appl. Opt.* **20**, 3477 (1981); and B. Yaakobi, J. A. Delettrez, L. M. Goldman, R. L. McCrory, W. Seka, and J. M. Soures, *Opt. Commun.* **41**, 355 (1982).
6. R. S. Craxton, R. L. McCrory, and J. M. Soures, *Sci. Am.* **255**, 68 (1986).
7. E. J. McGuire, in *Atomic Inner-Shell Processes*, edited by B. Crasemann (Academic Press, New York, 1975), Vol. I, pp. 293–330.
8. P. Auger, *J. Phys. Radium* **6**, 205 (1925).
9. H. U. Freund, *X-Ray Spectrometry* **4**, 90 (1975).
10. V. L. Jacobs and J. Davis, *Phys. Rev. A* **18**, 697 (1978).
11. D. Duston, J. E. Rogerson, J. Davis, and M. Blaha, *Phys. Rev. A* **28**, 2968 (1983).
12. R. Epstein, *Phys. Rev. A* **43**, 961 (1991).